

## Article

# Mechanical Properties of Cold Sprayed Aluminium 2024 and 7075 Coatings for Repairs

Jiawei Kelvin Bi <sup>1,\*</sup>, Zhi Cheng Kelvin Loke <sup>2,\*</sup>, Chi Keong Reuben Lim <sup>1</sup>, Kok Hoon Tony Teng <sup>2</sup> and Pak Keng Koh <sup>2</sup>

<sup>1</sup> Republic of Singapore Air Force, Singapore 534236, Singapore; LIM\_Chi\_Keong\_Reuben@defence.gov.sg

<sup>2</sup> ECK Pte Ltd., Singapore 797547, Singapore; tonyteng@eckpl.com (K.H.T.T.); pkkoh@eckpl.com (P.K.K.)

\* Correspondence: BI\_Kelvin@defence.gov.sg (J.K.B.); kelvinloke@eckpl.com (Z.C.K.L.)

**Abstract:** This study investigates the mechanical properties of aluminium 2024 (Al-2024) and aluminium 7075 (Al-7075) cold-sprayed materials and coatings for repairs. It aims to determine the acceptable data needed to meet regulatory requirement when substantiating cold spray repairs. The study focuses on repairs of non-principal structural element (PSE) structures such as skin and panels that are prone to corrosion and wear. For cold spray repair of such components, the microstructure, tensile, peel, bearing, and bending strength from the repair process and powder materials of Al-2024 and Al-7075, were identified and investigated in accordance with MIL-STD-3021. Results show an average coating porosity of <1.2% for both materials. Average tensile strength was 247.1 MPa (with elongation of 0.76%) for Al-2024 and 264.0 MPa (with elongation of 0.87%) for Al-7075. Al-2024 has an average peel strength of 71.9 MPa, while Al-7075 is at 48.9 MPa. The Al-2024 bearing test specimens gave a maximum load strength before failure of 633.6 MPa, while the Al-7075 gave 762.7 MPa. The bending tests show good flexibility for coating thickness ranges of typical skin and panel parts. The results show that cold spray can be used to restore thickness and oversized hole diameters for Al-2024 and Al-7075 skin and panels. The bearing test conducted in this study has also demonstrated a new test method to determine the bearing load and yield strength of a cold spray-repaired hole in a plate.

**Keywords:** cold spray; repair; remanufacturing; aluminium; coating microstructure; mechanical properties



**Citation:** Bi, J.K.; Loke, Z.C.K.; Lim, C.K.R.; Teng, K.H.T.; Koh, P.K. Mechanical Properties of Cold Sprayed Aluminium 2024 and 7075 Coatings for Repairs. *Aerospace* **2022**, *9*, 65. <https://doi.org/10.3390/aerospace9020065>

Academic Editor: Khamis Essa

Received: 13 December 2021

Accepted: 21 January 2022

Published: 26 January 2022

**Publisher's Note:** MDPI stays neutral with regard to jurisdictional claims in published maps and institutional affiliations.



**Copyright:** © 2022 by the authors. Licensee MDPI, Basel, Switzerland. This article is an open access article distributed under the terms and conditions of the Creative Commons Attribution (CC BY) license (<https://creativecommons.org/licenses/by/4.0/>).

## 1. Introduction

Cold spray is a spray deposition process which uses high-velocity gases (the commonly used gases are compressed air, nitrogen, and helium) to deposit metal powders from a “de Laval” nozzle with a converging-diverging internal geometry at velocities of more than Mach 1 [1,2]. Research has shown that build-up is successful only when the powder particles were able to attain a certain “critical velocity” prior their impact on the substrate surface [3]. This critical velocity is dependent on several equipment parameters such as gas pressure and gas temperature, as well as material properties such as powder morphology and metallurgy [2]. A mixture of mechanisms were believed to be responsible for the bonding of coatings, mainly mechanical interlocking and metallurgical bonding due to adiabatic shear instability at powder particle–substrate interface [3–5]. Recent reports have been made on the investigation into the roles of mechanical interlocking and adiabatic shear instability in cold spray bonding mechanisms, and has presented contradictory hypotheses which will require further investigations [6–8]. The amount of interfacial bonded material sprayed at varying angles was also investigated and found to decrease with increasing spray angles [9]. Previous works have shared on the topic of potential cold spray applications, especially in the field of aerospace materials, remanufacturing and additive manufacturing. Examples include the application of amorphous aluminium coatings deposited using cold spray for the corrosion protection of aluminium structures [10]. The repair-specific qualification for the U.S. Army’s magnesium rotorcraft components detailed the mechanical

and chemical tests carried out over small sample sizes [11]. Work was also reported on the effects of heat treatment on cold-sprayed tensile bars to replicate repaired parts [12,13]. This similar approach was observed in other aluminium cold spray repair substantiation with favourable results [14,15]. Work has also been reported to demonstrate the tests performed to characterise a cold-sprayed material and the cold spray process as an additive process for repair and manufacturing applications on stress-loaded parts [16]. A new axial fatigue test specimen design was also proposed to substantiate the fatigue performance of cold spray repair on a localised cavity [17,18]. With the release of USAF Structures Bulletin EZ-19-01 and the consideration of existing military standards (MIL-STD-1530D and JSSG-2006), a few applicability studies of Hartman-Schijve crack growth for cold spray repairs showed promising correlation with experimental data for durability and damage tolerance analysis (DADTA) [19–21]. However, these papers were for specific components and conducted with less than eight sample sizes in controlled environments. There is a lack of reliable cold spray material databases that can aid the in-field engineers with quick substantiation of their repair designs beyond dimension restoration.

In the referenced literature above, there has been extensive work done on the investigation of the cold spray bonding and consolidation mechanisms, materials that can be cold sprayed, behaviour of these materials to post-processes like heat treatment, various methods of material characterisation, and the types of applications that cold spray may be applied to. The work done and reported in open literature has not adequately addressed the gap in aviation standards regulating the application of cold spray in aviation component repair. This is the motivation behind this work, which is meant to be a starting point in helping to address this gap.

The Federal Aviation Administration (FAA)-defined “acceptable data” offers the fastest response for minor repairs vis-à-vis “approved data” [22]. Limited efforts to substantiate cold spray repair in compliance with FAA’s extensive process for generic repair on commercial aircraft were noted [23,24]. Hence, the industry requires further studies to establish a cold spray database similar to the Metallic Materials Properties Development and Standardization (MMPDS) in accordance with industry repair standards. This work aims to provide a starting point in acting as a guide and precedent in outlining the testing methodology and also some reference data specifically for aluminium 2024 and 7075 cold-sprayed materials, while the database is still to be established.

This study investigated the mechanical properties of Al-2024 and Al-7075 cold-sprayed materials and coatings, with the intent to build up adequate understanding and data for cold spray repair, guided by the European Union Aviation Safety Agency’s (EASA) Part 21 requirements. The testing approach used in this work was designed to provide the necessary data and confidence through a larger sample size. The desired outcome is to eventually implement cold spray for low-risk repairs, such as corroded panels and enlarged holes on aviation platforms.

## 2. Repair Candidate and Technical Data Requirements

The repair candidate selected in this study is a typical sheet metal assembly with a fastener joint as shown in Figure 1. Such an assembly is commonly found on aircraft skin, panels, brackets and stiffeners and is prone to surface corrosion and fastener hole wear. When the corrosion depth of the sheet metal or fastener hole enlargement exceeds stipulated limits, these parts need to be replaced. Cold spray repair can be an economical alternative to replacement by restoring the dimensions and load-bearing capability of the part. For approval of such a repair, acceptable technical data is required to substantiate the repair design. In this work, low risk parts with low load-bearing requirements which are not fatigue critical are targeted. The key relevant regulations applicable to the types of repairs are:

- EASA CS25.603—Materials: Assurance of material sources and handling,
- EASA CS25.605—Fabrication methods: Assurance of fabrication process and controls, and



- EASA CS25.613—Material design values: Determination of statistically significant design values that considers variability introduced in material and fabrication.

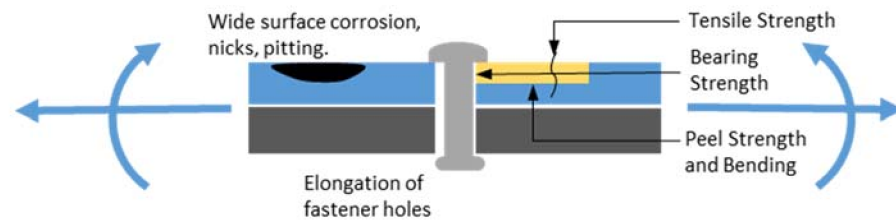


**Figure 1.** Schematic illustration showing defects on a typical skin panel or bracket.

Based on these requirements, the identified technical data required for cold spray repair are (1) the microstructure examination to assure reliability and (2) the tensile, peel, bearing and bending strength from the repair process and powder materials. As the parts are typically Al-2024 and Al-7075 alloys, the performance of the cold spray repair for both materials are investigated.

### 3. Material and Repair Process

Al-2024 and Al-7075 are the primary materials investigated due to their common usage in the aviation industry. The powders used for cold spraying are commercially available aluminium 2024 (AM 2024) and aluminium 7075 (AM 7075) alloys from Valimet Inc. (Stockton, CA, USA) with a spherical-morphology and average diameter of 30–33  $\mu\text{m}$ . Al-2024-T351 and Al-7075-T6511 were used as the corresponding substrates. The powder storage and handling procedures in this work were adhered to ECK's Quality Management System. The cold spray process used to produce these samples was per ECK work instructions ECK WI-002.

### 4. Cold Spray Process

The cold spray equipment used in this work is the commercially-available Series P low-pressure cold spray system from Centreline (Windsor Limited, Windsor, ON, Canada). The spray nozzle had a stand-off distance of 25 mm and travelled at 30 mm/s. Helium was used as the carrier gas at 0.965 MPa and 400 °C.

## 5. Experiment for Material Design Value

### 5.1. Test Methodology

The following material tests (Table 1) were selected based on the types of defects and subsequent repair methods prescribed and the examples provided in MIL-STD-3021 (July 2011) Appendix A for structural applications and ASTM standards. This is to provide the required material information to qualify the cold spray process and material for the intended repair application described in Section 2.

**Table 1.** Reference Standards for Material Properties.

No.	Reference Standard	Material Property to Be Determined
1	ASTM E3	Inherent flaws and defects within the cold-sprayed coating
2	ASTM E8	Tensile strength of cold-sprayed material
3	ASTM C633	Peel strength of the cold-sprayed coating
4	ASTM E290	Deformation and bending strength of the cold-sprayed coating
5	ASTM E238	Fastener bearing strength of the cold-sprayed coating

The quantity of 20 coupons made from a single lot of powder for each alloy were used for each test. While MIL-STD-3021 stated a minimum of 3 test specimens, a higher number of 20 coupons was adopted such that a larger statistical basis can be determined. It is recognised that it is still lower than the 30 samples required for S-Basis in accordance with MMPDS, and this is assessed to be acceptable for low-risk part applications targeted in this work.

## 5.2. Coating Specimen Preparation

### 5.2.1. Microstructure Test (ASTM E3)

For coating microstructure analysis, 25 mm thick Al-2024 and Al-7075 coatings measuring 40 mm (L) × 40 mm (W) were cold sprayed onto Al-2024 and Al-7075 substrates, respectively. For each material, a total of 20 different microstructure cross-sections, as shown in Figure 2, were made. The cross-sectioned coatings were polished and analysed under the microscope. Keller's reagent was used to etch the samples. Coating porosity study was conducted using an image analysis software. From the microstructure analysis of 20 different coating locations, the coatings were consistently 25 mm or more in thickness.

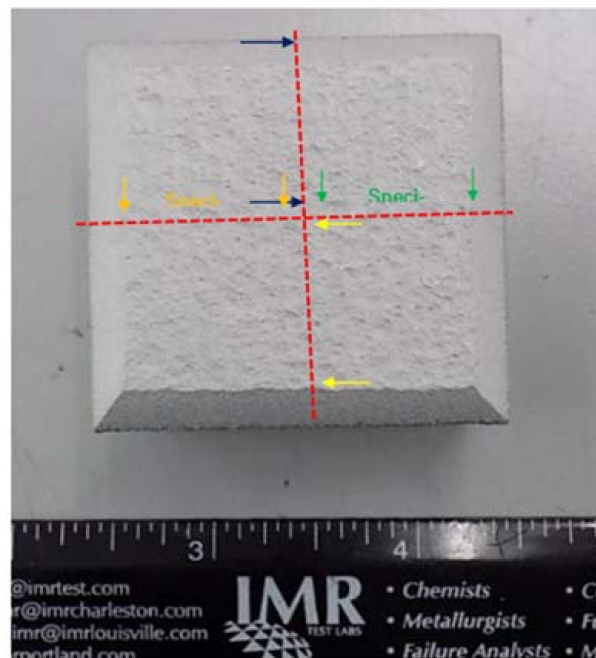


**Figure 2.** Specimen extraction for the microstructure analysis for the Al-2024 samples.

### 5.2.2. Tensile Test (ASTM E8)

For tensile strength testing, approximately 4 mm thick Al-2024 and Al-7075 coatings were cold-sprayed onto Al-2024 and Al-7075 substrates, respectively. The coatings were removed from the substrates using the wire-cut process. The coatings were further machined to the sub-size test specimen specifications as described in ASTM E8. An example of this specimen is shown in Figure 3. Twenty specimens were produced for each aluminium alloy.

### 5.2.3. Tensile Adhesion Test (ASTM C633)

The tensile adhesion or cohesion strength of the coatings were evaluated in accordance to the ASTM C633 test method. Al-2024 and Al-7075 coatings measuring 25 mm thick and 25 mm in diameter were cold sprayed onto Al-2024 and Al-7075 substrates, respectively. Twenty specimens were produced for each aluminium alloy with some of the specimens shown in Figure 4.

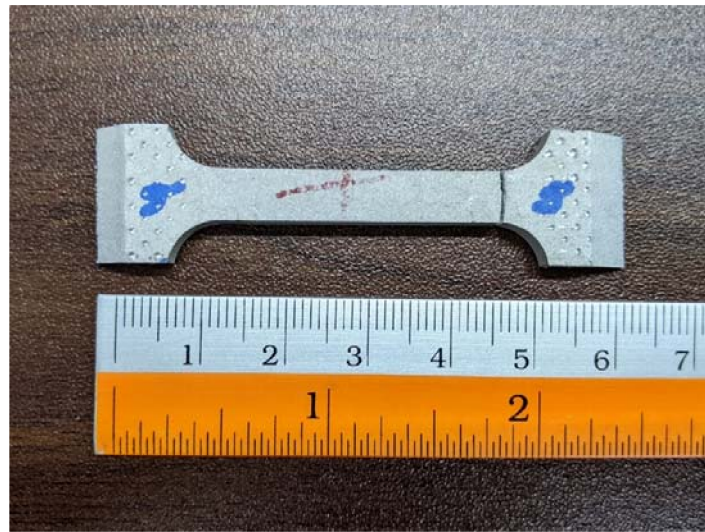


**Figure 3.** An example of the tensile test specimen tested in this work. The photo was taken after testing to show the crack in the specimen.



**Figure 4.** Al-2024 coating test specimens submitted for the adhesive bond strength test. The top image shows the coating top surface, while the bottom image shows the uncoated studs on the bottom side.

#### 5.2.4. Bearing Test (ASTM E238)

The bearing strength of the coated plates was established in accordance with ASTM E238. Al-2024 and Al-7075 coatings were cold sprayed to fill up the 12 mm diameter through-holes made on Al-2024 and Al-7075 substrates, respectively. The substrates measured 150 mm (L) by 38 mm (W) by 5 mm (T). Subsequently, 6 mm diameter holes were drilled right in the middle of the cold-sprayed material for the test. Figure 5 shows the plates before drilling, with the 12mm diameter through-hole, and after cold spray. Twenty specimens were produced for each aluminium alloy.

The tests were performed at room temperature using servo-hydraulic fatigue frames (MTS Systems Corporation, Eden Prairie, MN, USA) per ASTM E238. The tests were initiated in bearing strain/displacement control at 0.05 bearing strain/minute using an extensometer or a crack-opening displacement (COD) gage. The specimen was assembled in a clevis for bearing in tension where the mid plane of the specimen passes through the line of action. One clip gage was attached to the specimen face to measure the hole deformation.

Ultimate bearing strength and bearing stress at 2% offset were calculated using the following equations:

$$\text{Ultimate Bearing Strength (psi)} = \frac{P_{Ult}}{dt} \quad (1)$$

$$\text{Bearing Strength at 2\% offset (psi)} = \frac{P_{2\%offset}}{dt} \quad (2)$$

where  $P_{Ult}$  = ultimate bearing load which is defined as the maximum load observed during testing (N),  $P_{2\%offset}$  = bearing load at 2% offset (oad at the point where the intersection of the stress vs. strain curve and a linear line which is drawn parallel to the initial linear portion of the stress vs. hole deformation curve and shifted by 2% hole deformation) (N),  $d$  = pin diameter (mm), and  $t$  = measured thickness (mm).



**Figure 5.** The left-most plate shows the substrate before drilling the hole. The substrate in the middle shows the location of the 12 mm diameter hole. The plate on the far right shows the hole after being filled up with cold-sprayed material and manually ground until flat on both sides.

#### 5.2.5. Bending Test (ASTM E290)

Bending test based on ASTM E290 was conducted to obtain the bending angles and displacements of the coating before failure. Cracking, breaking and/or delaminating constitute the failure of the coating. The thickness of the coatings varied from 0.457 to 1.524 mm, while the substrate's thickness ranged from 0.889 to 2.286 mm. The substrate's width is 10 mm and length is 200 mm. Test specimens are shown in Figure 6.



**Figure 6.** One set of aluminium 2024 bending test specimens (before bend testing).



According to the Guided-Bend with No-Die Test equation provided in ASTM E290, the top mandrel diameter was calculated to be 66 mm with the “C-spacing”. The distance between the two lower roller supports was 105 mm. The bend angle of the specimens at failure is derived with the bend angle to be equal to  $2\theta$ .

## 6. Results and Discussion

### 6.1. Microstructure Analysis

The average percentages of porosity measured from 20 readings of each coating were  $1.148 \pm 0.614\%$  for Al-2024 and  $0.006 + 0.009 - 0.006\%$  for Al-7075. This is in line with reports from other researchers and industrial releases on the porosity of cold-sprayed materials [6,7]. Micrographs of each representative coating are shown in Figures 7 and 8.

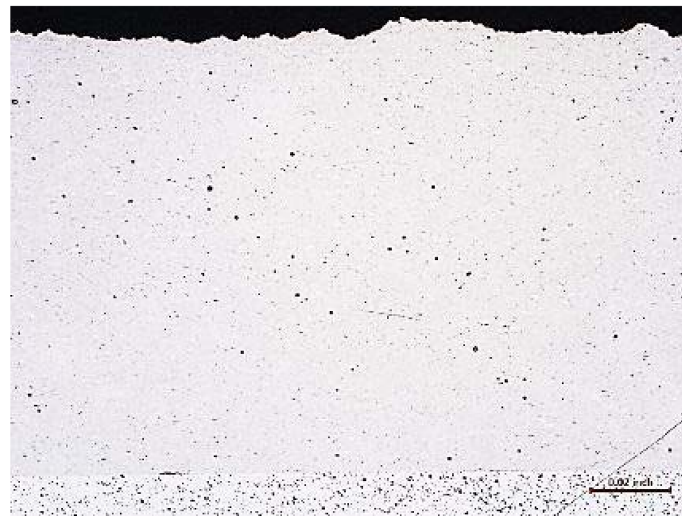


**Figure 7.** Micrograph depicting typical microstructure observed on aluminium 2024 cold-sprayed coating on aluminium 2024 substrate. As-etched; At  $25\times$ .



**Figure 8.** Micrograph depicting typical microstructure observed on aluminium 7075 cold-sprayed coating on aluminium 7075 substrate. As-etched; at  $25\times$ .

The purpose of the microstructural analysis was to determine the visual baseline of the cold-sprayed materials that were tested. This was done by establishing the porosity levels of the cold-sprayed materials. With this general understanding, the mechanical properties



obtained for these two cold-sprayed materials with the powder, equipment and parameters used can be correlated.

From the microstructure images of both Al-2024 and Al-7075 coatings, it can be deduced that the resultant Al-2024 and Al-7075 cold-sprayed materials are consistently dense, with an average porosity observed to be 1.15% or lower. There was also no observation of cracks within the cold-sprayed materials. This is consistent with the general understanding about cold-sprayed aluminium materials from Loke et al. [9] and Champagne [11].

As shown in Figure 9, there is a cold-worked grain structure within each highly deformed splat. This is formed by the extensive deformation of individual aluminium powder particles during the cold spray process. This highly stressed grain structure and the splats would give rise to the low elongation and ductility and is inherent to cold-sprayed materials. It is possible to alter this microstructure by prescribing heat treatment such as annealing and solid-state solution [12,13].



**Figure 9.** Micrograph depicting the typical microstructure observed on Al-2024 cold-sprayed coating on Al-2024 substrate. As-etched; at 100 $\times$ .

### 6.2. Tensile Strength

The average tensile strength of the Al-2024 cold-sprayed material was found to be  $247 \pm 57$  MPa ( $35 \pm 8$  ksi), and  $264 \pm 56$  MPa ( $38 \pm 8$  ksi) for Al-7075. The average elongations were  $0.77 \pm 0.90\%$  for Al-2024 and  $0.87 \pm 0.90 - 0.87\%$  for Al-7075. These results are broadly in agreement with reports from Loke et al. [9] and Koh et al. [10] that cold-sprayed material will possess low elongation without heat treatment. The tensile strength results in histogram and normal distribution curves for both aluminium alloys are shown in Figure 10. The average strength values and strength reference from MMPDS were added for comparison.

The purpose of the tensile test is to determine the tensile strength and elongation of the cold-sprayed materials. This was done by cold spraying thick coatings and subsequently machining tensile test specimens from the coating material for testing.

Tensile strength was found to be of an average of 247 MPa (elongation 0.76%) for Al-2024 and 264 MPa (elongation 0.87%) for Al-7075. These values were compared with the AMS 4037 and AMS 4045 values for Al-2024 T3 and Al-7075 T6 sheets, which are 269 MPa (elongation 10%) and 469 MPa (elongation 8%), respectively. The cold-sprayed Al-2024 and Al-7075 coatings are at 92.0% and 56.3% of the tensile strength of their respective sheet material. The results for both materials are normally distributed with no skew towards either end.

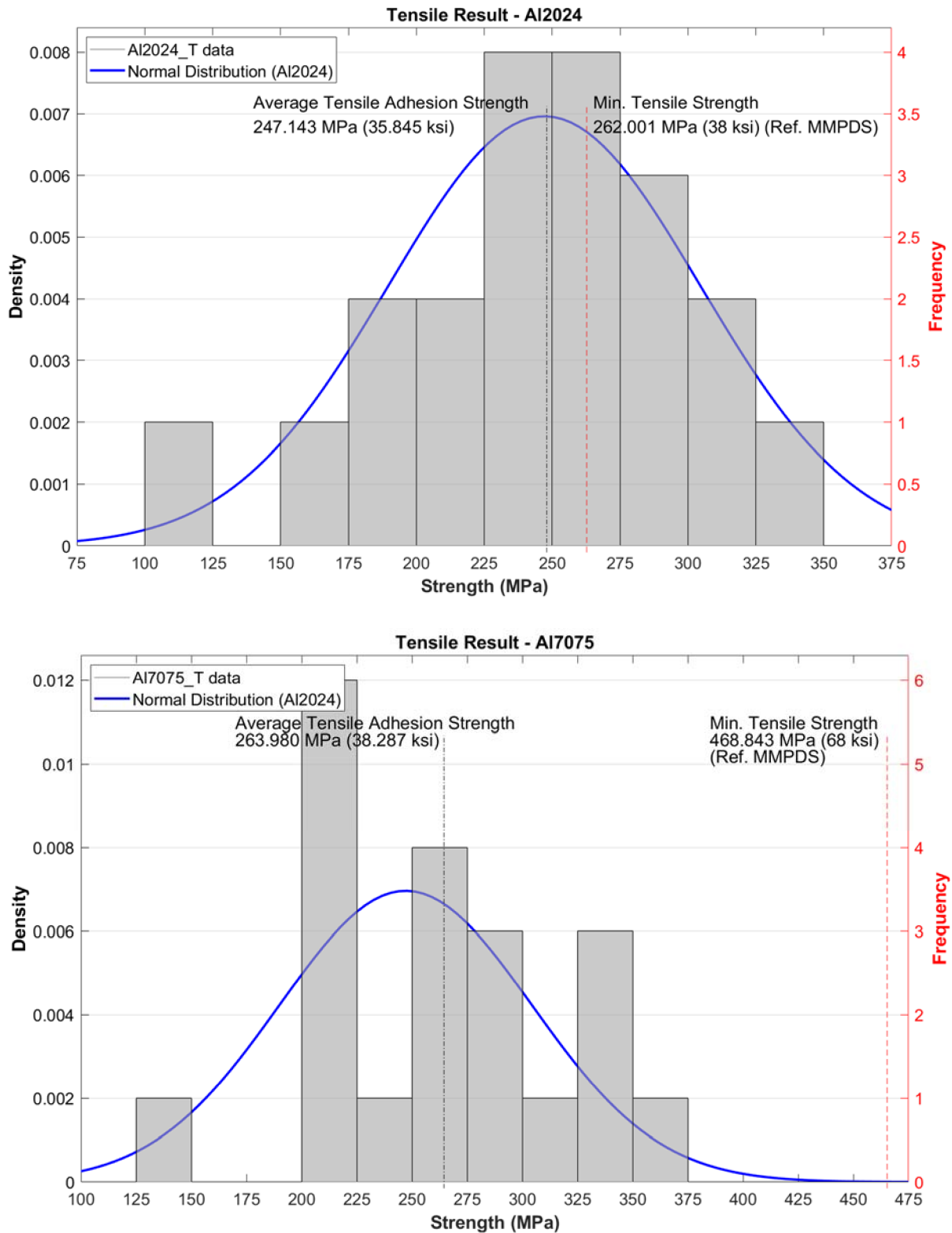


**Figure 10.** Normal distribution histogram and curve of the tensile strength results of both cold-sprayed Al-2024 and Al-7075 coating materials.

The results are consistent with expectations based on the microstructural characteristics described in Section 6.1. The better performance from Al-2024 could be attributed to its lower tensile strength and hardness relative to Al-7075, which could promote more ductile

behaviour when the powder underwent plastic deformation during deposition [14]. It should also be noted that the cold-sprayed specimens were not heat treated to T3 and T6 which was the condition in the AMS specifications. This would explain the lower readings compared to the MMPDS reference values. Heat treatment of the cold spray coatings to obtain the desired ductility remains an option for the repair. The relatively high tensile strength results, especially for Al-2024, provided the confidence for the utilization of cold spray repair for skin thickness restoration.

### 6.3. Tensile Adhesive Bond Strength

The coatings demonstrated tensile adhesive bond strengths averaging  $71.9 \pm 15.0$  MPa for Al-2024 and  $48.9 \pm 14.0$  MPa for Al-7075. The failure locations were mainly either at the epoxy adhesive as illustrated in Figure 11 as failure “e”, or at the coating “c”. Figure 12 shows the normal distribution histogram and curve of the tensile adhesive bond strength results of both aluminium coatings. The average strength values and tensile strength of adhesive EA9309 were added for comparison.

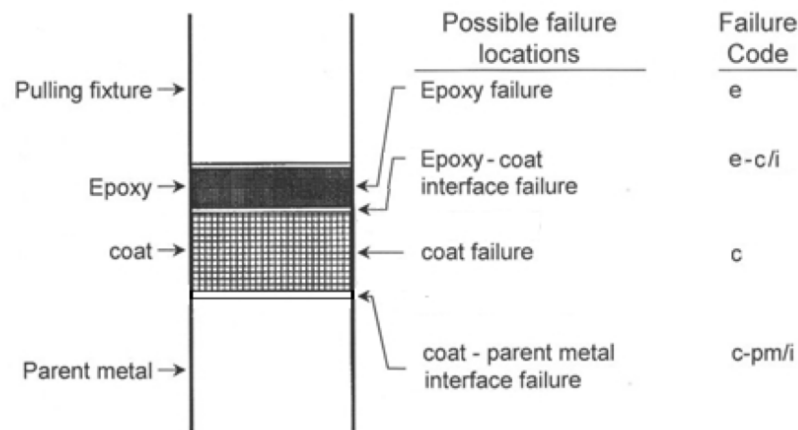


**Figure 11.** Schematic showing the different failure mode characterisations in the adhesive bond strength test.

The results for Al-2024 and Al-7075 were an average of 71.9 MPa and 48.9 MPa, respectively. As compared to adhesive EA9309 with a tensile strength of 31.0 MPa, the obtained average values were 131.7% (Al-2024) and 57.7% (Al-7075) higher.

The skewed distribution of the Al-2024 data shown in Figure 12 suggests that the two lower results could be outlining data, while the distribution curve for the Al-7075 results indicated a wider spread of the data points. Berndt [25] reported that the tensile adhesion bond strength test can be a highly variable test which is strongly influenced by the specimen preparation technique and is not a reliably reproducible material property. This is despite this test being the de-facto industrial test standard for thermal spray coatings due to its simplicity of implementation. Berndt did suggest that the testing should be performed until the coefficient of variance is less than 30% for the data set.

The purpose of the tensile adhesive bond strength test is to determine the tensile adhesive bond strength of the cold-sprayed coatings. This was done by cold spraying thick coatings for testing.

Based on Berndt’s suggestion, the coefficient of variance was calculated for the two bond strength tests conducted. The coefficient of variance for Al-2024 and Al-7075 were found to be below 30% at 21% and 29% respectively. This provided an enhanced level of confidence in the consistency of the results for this study.

The relatively high tensile adhesion test results obtained are consistent with the microstructure images of the coatings shown in Section 6.1. The well-defined interface between the coating and the substrate and the absence of defects and low porosity are clear indications of a high density coating which is strongly anchored to the substrates.

The correlated results provided the confidence that the tensile adhesion quality of the cold-sprayed coatings will adequately meet in-service stress loads.

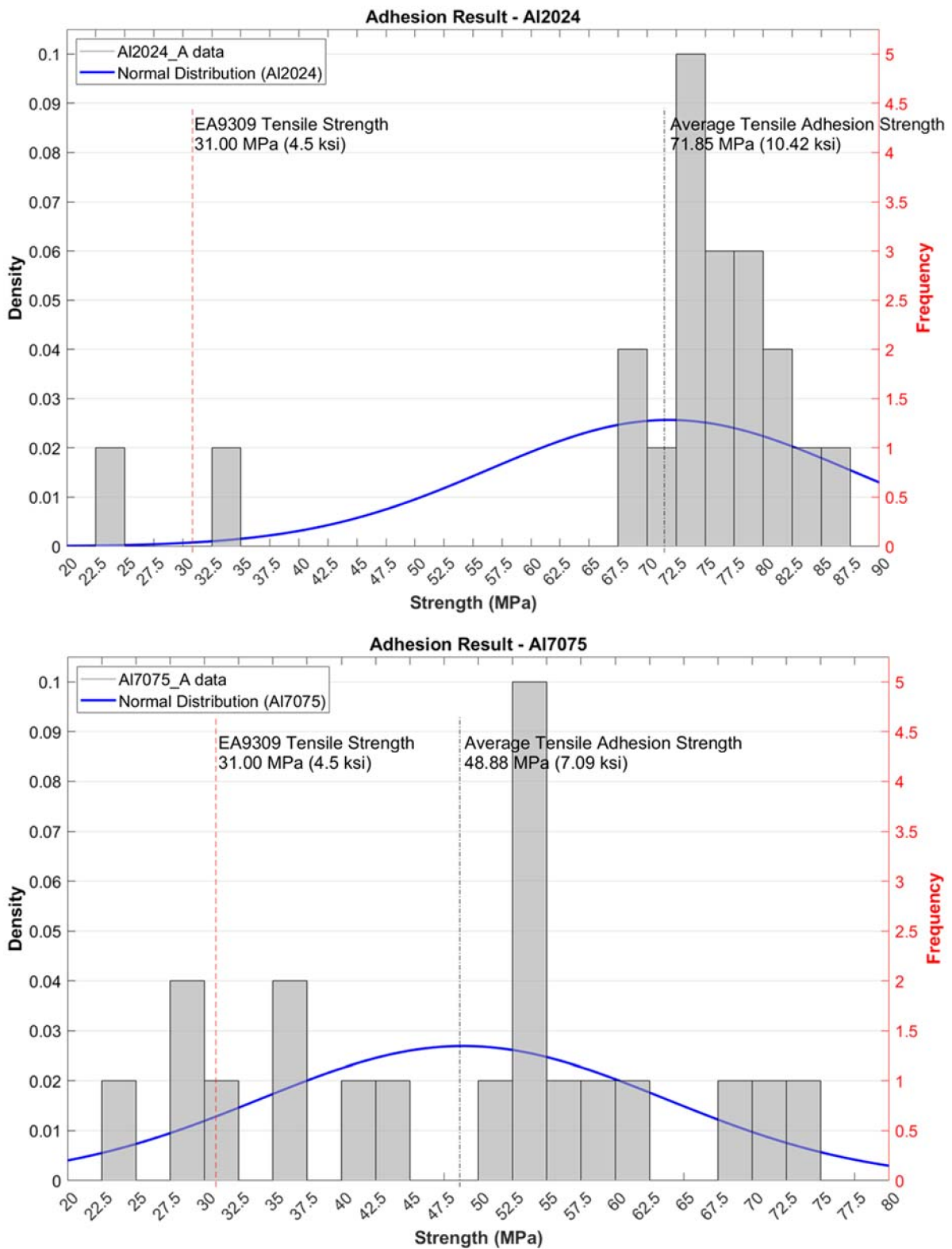
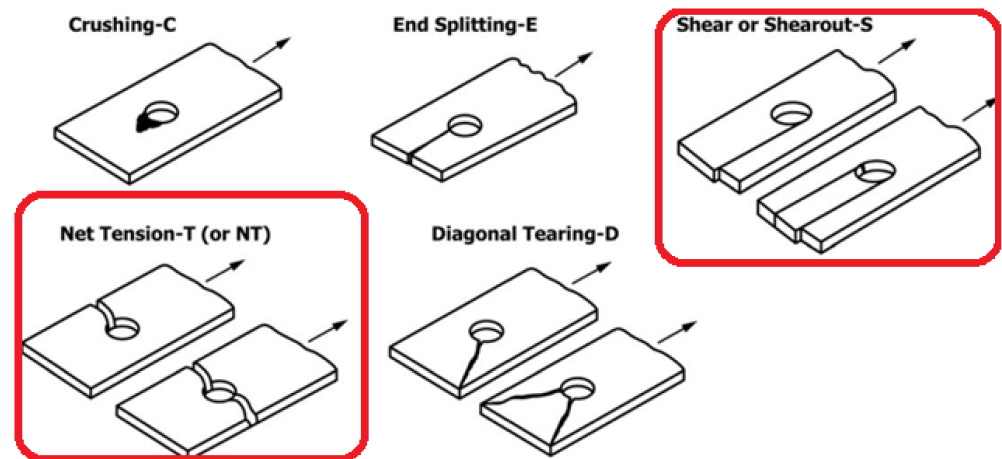


Figure 12. Normal distribution histogram and curve of the tensile adhesive bond strength results of both cold-sprayed Al-2024 and Al-7075 coatings.

#### 6.4. Bearing Test

The bearing test results gave an average of  $519 \pm 60$  MPa offset yield stress and  $634 \pm 48$  MPa peak stress for Al-2024. For Al-7075, the offset yield stress was  $678 \pm 19$  MPa, and peak stress was  $763 \pm 25$  MPa. All the test specimens demonstrated a failure mode of S + NT, as shown in Figure 13. The summarized average test results are shown in Table 2. Figure 14 shows the normal distribution histogram and curve of the bearing yield strength results for both aluminium alloy materials. The average value and minimum bearing strength reference from MMPDS were added for comparison.



**Figure 13.** Schematic illustrations showing the various failure modes from the bearing test.

**Table 2.** Summary of bearing strength test results.

Alu	Minimum Bearing Strength MPa (ksi) (Ref. MMPDS-01)	CS Offset Yield Stress MPa (ksi)	CS Peak Stress MPa (ksi)
2024	503 (73)	$519 \pm 60$ ( $75 \pm 9$ )	$634 \pm 48$ ( $92 \pm 7$ )
7075	710 (103)	$678 \pm 19$ ( $98 \pm 3$ )	$763 \pm 25$ ( $111 \pm 4$ )

The two failure modes noted in the test results are circled.

The purpose of the bearing test is to determine the maximum load-bearing tensile strength and yield strength of over-sized through-holes repaired by cold spraying on the inner diameter of the holes.

The Al-2024 test specimens gave an offset yield strength of 519 MPa, while the Al-7075 gave 677 MPa. Comparing with the AMS 4037 and AMS 4045 data of 503 MPa (0.01-0.128", Al-2024 T3 sheet) and 710 MPa (0.04-0.125", Al-7075 T6/T62 sheet), respectively, the yield strength of the cold-sprayed Al-2024 hole is 3.1% higher than the AMS 4037 requirement, while Al-7075 is 4.5% lower than the AMS 4045 specification. It is important to note that the cold-sprayed specimens were not heat treated to T3 and T6 conditions as stated in the AMS specifications.

The Al-2024 test specimens gave a peak load strength before failure of 634 MPa, while the Al-7075 gave 763 MPa. Comparing with the AMS 4037 and AMS 4045 data of 503 MPa (0.01-0.128", Al-2024 T3 sheet) and 710 MPa (0.04-0.125", Al-7075 T6/T62 sheet), the maximum load strength of both cold-sprayed Al-2024 and 7075 holes are higher than the AMS 4037 and 4045 requirements. Incidentally, the cold-sprayed specimens were also not heat treated to T3 and T6 conditions as stated in the AMS specifications.

From both results, it can be implied that cold spray can be used to restore oversized hole diameters for Al-2024 and Al-7075 panels with comparable strengths to meet AMS 4037 and 4045 specifications, respectively.



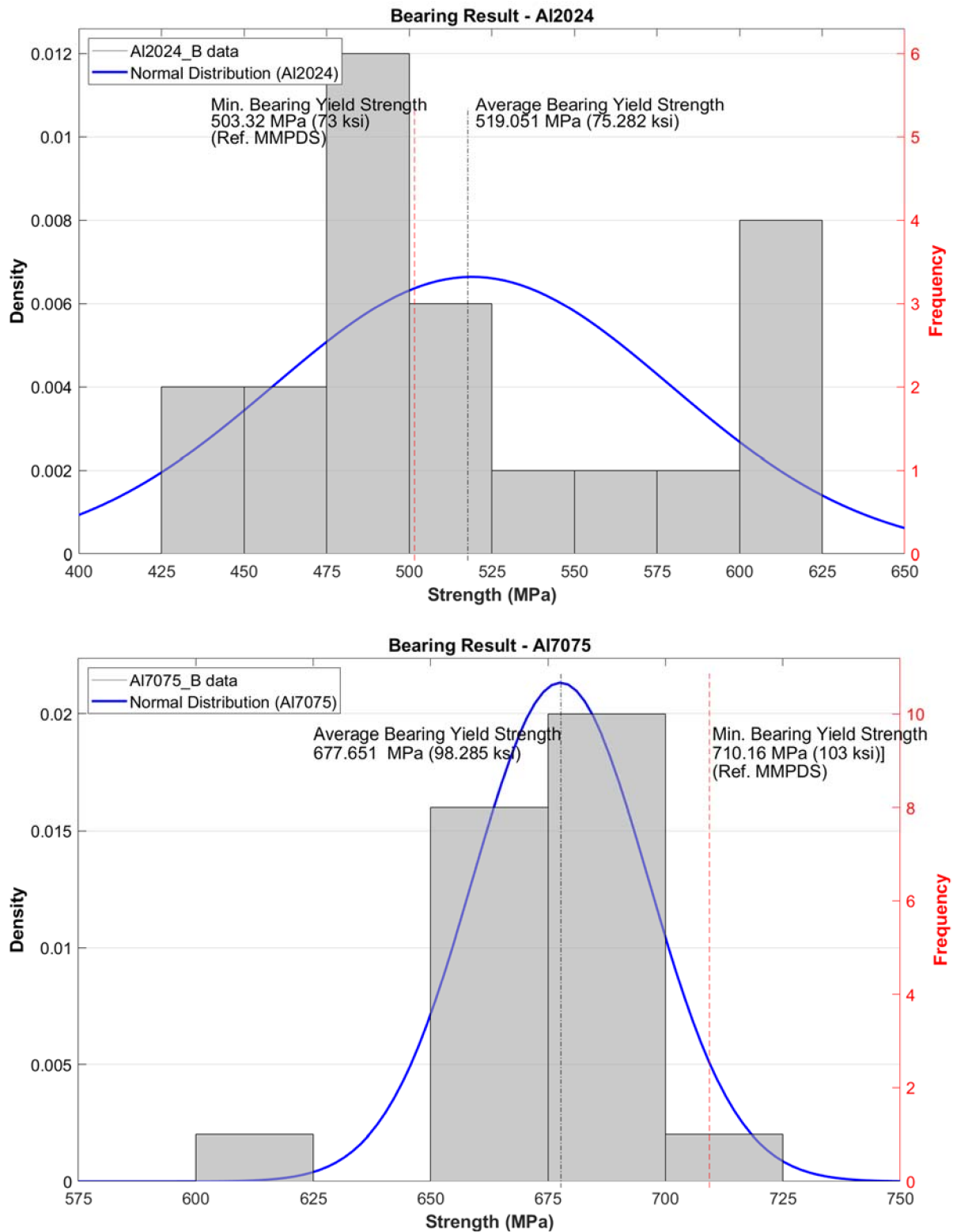


**Figure 14.** The normal distribution histogram and curve of the bearing strength results of both cold-sprayed Al-2024 and Al-7075 coating materials.

**6.5. Bending Test**

The coating and substrate thicknesses were selected based on the types of panels that were down-selected for repair using cold spray. From Figures 15–17, it is notable that the

0.457 mm (0.018") Al-2024 and Al-7075 coatings demonstrated significantly higher coating flexibility compared to the other specimen sets. In addition, there is a general observation of low flexibility in Al-2024 and Al-7075 coatings, with a maximum bending displacement below 10 mm and a maximum bend angle below 35° before coating failure was observed.

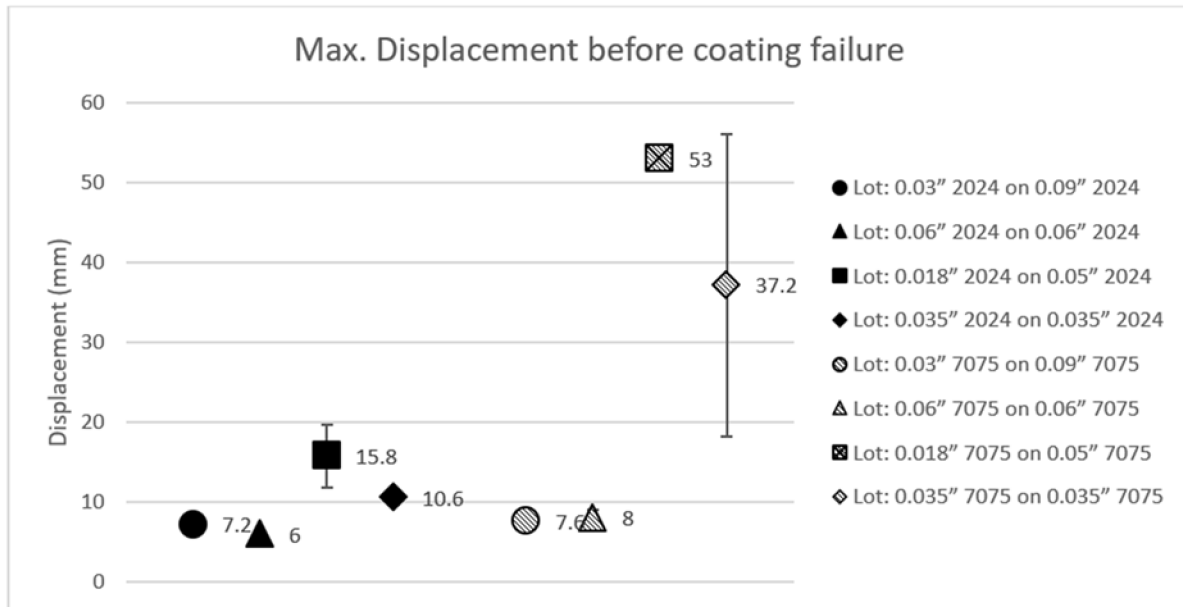


Figure 15. Averaged maximum displacement from the horizontal plane before coating failure.

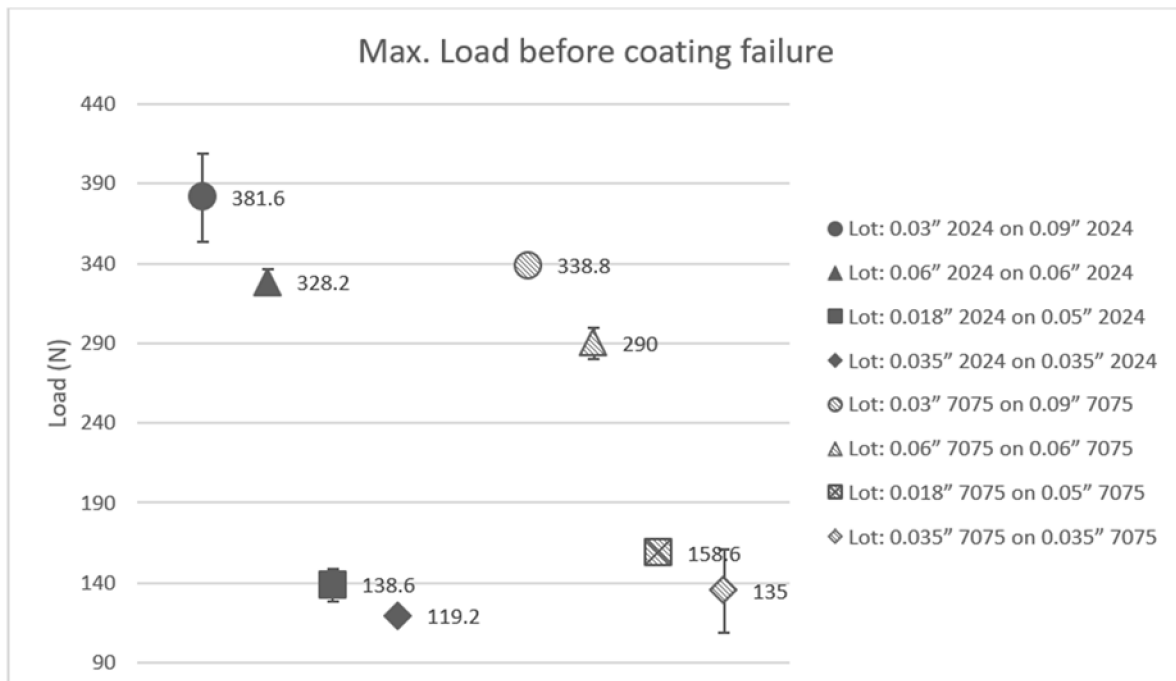
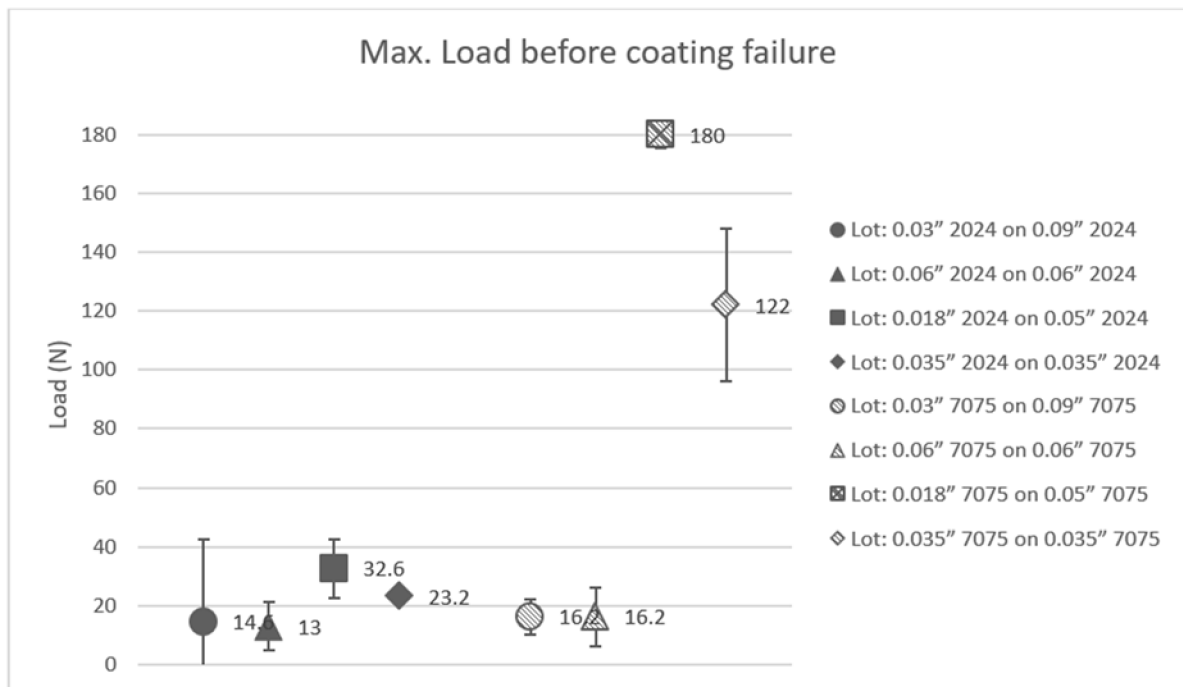


Figure 16. Averaged maximum load on the coating before coating failure.

The purpose of the bending test is to establish the maximum degree angle of bending the cold-sprayed coatings can be subjected to before failure. From the results presented in Figures 15–17, it was observed that there is a general trend of decreasing coating flexibility (angle before coating failure) with increasing coating thickness. There is also an observation

that the substrate thickness could influence the coating flexibility, with a thicker substrate causing thin coatings to fail at lower bend angles. The minimum bend angle of 12° and 14° were observed on thin coatings of Al-2024 and Al-7075, respectively, and gave the confidence of the coatings' performance and adequacy to meet in-service loads.



**Figure 17.** Averaged maximum bend angle from the horizontal plane before coating failure.

## 7. Conclusions

This study investigated the mechanical properties of aluminium 2024 (Al-2024) and aluminium 7075 (Al-7072) cold-sprayed coatings. Based on the types of defects and intended repair methods, the following material properties were identified to be key for the successful qualification of the repair process and powder materials used.

- The average percentage of coating porosity measured was 1.148% for Al-2024 and 0.006% for Al-7075. Tensile strength was found to be of an average of 247 MPa (elongation 0.77%) for Al-2024 and 264 MPa (elongation 0.87%) for Al-7075. These values were compared with the AMS 4037 and AMS 4045 values for Al-2024 T3 and Al-7075 T6 sheets, which are 269 MPa (elongation 10%) and 469 MPa (elongation 8%), respectively. Al-2024 was able to provide an average tensile adhesion bond strength of 72 MPa, while Al-7075 had an average of 49 MPa.
- The Al-2024 test specimens gave a bearing offset yield strength of 519 MPa, while the Al-7075 gave 678 MPa. The Al-2024 test specimens gave a peak load strength before failure of 634 MPa, while the Al-7075 gave 763 MPa. The cold-sprayed specimens were not heat treated to the T3 and T6 conditions stated in the AMS specifications. Thus, the readings obtained were assessed to be adequate for oversized hole diameter restoration when the cold-sprayed coatings are heat treated per AMS 4037 and AMS 4045.
- It was observed that there is a general trend of decreasing coating flexibility (angle before coating failure) with increasing coating thickness. There was also an observation that the substrate thickness could influence the coating flexibility, with a thicker substrate causing thin coatings to fail at lower bend angles.

The results obtained in this study provided adequate data to substantiate the implementation of cold spray to restore thickness and oversized hole diameters for Al-2024 and Al-7075 skin and panels. In addition, the bearing test has demonstrated a new test method

to determine the bearing load and yield strength of a cold spray-repaired hole in a plate. Future studies can examine the mechanical behaviours of cold spray repair subjected to in-field loading to ascertain the repair adequacy. Parametric investigation of the spray parameters to improve the coating quality can be an alternative means to heat treatment which can have limited in-field application. The test scope of the current study can also be adopted for other materials to expand the database.

**Author Contributions:** Conceptualization, J.K.B. and Z.C.K.L.; methodology, J.K.B., C.K.R.L. and Z.C.K.L.; formal analysis, J.K.B., Z.C.K.L. and P.K.K.; resources, K.H.T.T.; data curation, J.K.B. and Z.C.K.L.; writing—original draft preparation, Z.C.K.L. and J.K.B.; writing—review and editing, C.K.R.L. and P.K.K.; visualization, J.K.B. and Z.C.K.L.; supervision, C.K.R.L. and P.K.K.; project administration, J.K.B.; funding acquisition, J.K.B. All authors have read and agreed to the published version of the manuscript.

**Funding:** The authors would like to acknowledge the Government of the Republic of Singapore and the Republic of Singapore Air Force for funding and supporting this work under Contract Number 9020203419.

**Institutional Review Board Statement:** Not applicable.

**Informed Consent Statement:** Not applicable.

**Data Availability Statement:** The data presented in this study are available on request from the corresponding author. The data are not publicly available due to contractual obligations from the funding authority. The data may be released upon request, with the written approval from the authors and the institutions that they represent.

**Acknowledgments:** The authors would also like to acknowledge Adrian Chua, staff officer from the Republic of Singapore Air Force, for his involvement in preparing the histograms presented in this manuscript.

**Conflicts of Interest:** The authors declare no conflict of interest.

## References

1. Davis, J.R. (Ed.) *Handbook of Thermal Spray Technology*; ASM International: Almere, The Netherlands, 2004; p. 77.
2. Papyrin, A.; Kosarev, V.; Klinkov, S.; Alkimov, A.; Fomin, V.M. *Cold Spray Technology*; Elsevier: Amsterdam, The Netherlands, 2006; pp. 1–32.
3. Kumar, S.; Bae, G.; Lee, C. Deposition characteristics of copper particles on roughened substrates through kinetic spraying. *Appl. Surf. Sci.* **2009**, *255*, 3472–3479. [[CrossRef](#)]
4. Grujicic, M.; Zhao, C.L.; DeRosset, W.S.; Helfritsch, D. Adiabatic shear instability based mechanism for particles/substrate bonding in the cold-gas dynamic-spray process. *Mater. Design* **2004**, *25*, 681–688. [[CrossRef](#)]
5. Assadi, H.; Gärtner, F.; Stoltenhoff, T.; Kreye, H. Bonding mechanism in cold gas spraying. *Acta Mater.* **2003**, *51*, 4379–4394. [[CrossRef](#)]
6. Hassani-Gangaraj, M.; Veysset, D.; Champagne, V.K.; Nelson, K.A.; Schuh, C.A. Adiabatic shear instability is not necessary for adhesion in cold spray. *Acta Mater.* **2018**, *158*, 430–439. [[CrossRef](#)]
7. Singh, S.; Singh, H.; Buddu, R.K. Microstructural investigations on bonding mechanisms of cold-sprayed copper with SS316L steel. *Surf. Eng.* **2020**, *36*, 1067–1080. [[CrossRef](#)]
8. Singh, S.; Raman, R.K.S.; Berndt, C.C.; Singh, H. Influence of Cold Spray Parameters on Bonding Mechanisms: A Review. *Metals* **2021**, *11*, 2016. [[CrossRef](#)]
9. Loke, K.; Zhang, Z.-Q.; Narayanaswamy, S.; Koh, P.K.; Luzin, V.; Gnaupel-Herold, T.; Ang, A.S.M. Residual Stress Analysis of Cold Spray Coatings Sprayed at Angles Using Through-thickness Neutron Diffraction Measurement. *J. Therm. Spray Technol.* **2021**, *30*, 1810–1826. [[CrossRef](#)]
10. Koh, P.K.; Cheang, P.; Loke, K.; Yu, S.C.M.; Ang, S.M. Deposition of amorphous aluminium powder using cold spray. In *International Thermal Spray Conference and Exposition—Air, Land, Water and the Human Body: Thermal Spray Science and Applications, ITSC 2012*; ASM International: Almere, The Netherlands, 2012; pp. 249–253.
11. Champagne, V.K. The Repair of Magnesium Rotorcraft Components by Cold Spray. *J. Fail. Anal. Prev.* **2008**, *8*, 164–175. [[CrossRef](#)]
12. Qiu, X.; Wang, J.-Q.; Gyansah, L.; Zhang, J.-X.; Xiong, T.-Y. Effect of Heat Treatment on Microstructure and Mechanical Properties of A380 Aluminum Alloy Deposited by Cold Spray. *J. Therm. Spray Technol.* **2017**, *26*, 1898–1907. [[CrossRef](#)]
13. Rokni, M.R.; Widener, C.A.; Ozdemir, O.C.; Crawford, G.A. Microstructure and mechanical properties of cold sprayed 6061 Al in As-sprayed and heat treated condition. *Surf. Coat. Technol.* **2017**, *309*, 641–650. [[CrossRef](#)]

14. Sirvent, P.; Garrido, M.A.; Munez, C.J.; Poza, P.; Vezzu, S. Effect of higher deposition temperatures on the microstructure and mechanical properties of Al 2024 cold sprayed coatings. *Surf. Coat. Technol.* **2018**, *337*, 461–470. [[CrossRef](#)]
15. Petráčková, K.; Kondás, J.; Guagliano, M. Mechanical Performance of Cold-Sprayed A357 Aluminum Alloy Coatings for Repair and Additive Manufacturing. *J. Therm. Spray Technol.* **2017**, *26*, 1888–1897. [[CrossRef](#)]
16. Widener, C.A.; Carter, M.J.; Ozdemir, O.C.; Hrabec, R.H.; Hoiland, B.; Stamey, T.E.; Champagne, V.K.; Eden, T.J. Application of High-Pressure Cold Spray for an Internal Bore Repair of a Navy Valve Actuator. *J. Therm. Spray Technol.* **2016**, *25*, 193–201. [[CrossRef](#)]
17. Petráčková, K.; Kondás, J.; Guagliano, M. Fixing a hole (with cold spray). *Int. J. Fatigue* **2018**, *110*, 144–152. [[CrossRef](#)]
18. Cavaliere, P.; Silvello, A. Crack Repair in Aerospace Aluminum Alloy Panels by Cold Spray. *J. Therm. Spray Technol.* **2017**, *26*, 661–670. [[CrossRef](#)]
19. Jones, R.; Matthews, N.; Peng, D.; Raman, R.K.S.; Phan, N. Experimental Studies into the Analysis Required for the Durability Assessment of 7075 and 6061 Cold Spray Repairs to Military Aircraft. *Aerospace* **2020**, *7*, 119. [[CrossRef](#)]
20. Kundu, S.; Jones, R.; Peng, D.; Matthews, N.; Alankar, A.; Raman, S.R.K.; Huang, P. Review of Requirements for the Durability and Damage Tolerance Certification of Additively Manufactured Aircraft Structural Parts and AM Repairs. *Materials* **2020**, *13*, 1341. [[CrossRef](#)] [[PubMed](#)]
21. Peng, D.; Tang, C.; Matthews, N.; Jones, R.; Kundu, S.; Raman, R.K.; Alankar, A. Computing the Fatigue Life of Cold Spray Repairs to Simulated Corrosion Damage. *Materials* **2021**, *14*, 4451. [[CrossRef](#)] [[PubMed](#)]
22. Johnson, D.; Lockhart, R. Approved versus acceptable repair data: How to make sure you have what you need. *Boeing Aero Quart.* **2007**, *Q3*, 6–13.
23. Fawaz, S. Substantiation process of cold spray repaired parts. In Proceedings of the Cold Spray Action Team Workshop 2017, Boston, MA, USA, 14–15 June 2017.
24. Dorman, S.; Fawaz, S. FAA certification of cold spray dimensional repair. In Proceedings of the Cold Spray Action Team Workshop 2019, Worcester, MA, USA, 25–26 June 2019.
25. Berndt, C.C. Tensile adhesion testing methodology for thermally sprayed coatings. *J. Mater. Eng.* **1990**, *12*, 151–158. [[CrossRef](#)]